Electronic Supporting Information

Role of polymeric surfactant in the synthesis of cobalt molybdate nanospheres for hybrid capacitor applications

Maryam Jozegholami Barmi and Manickam Minakshi Sundaram*

School of Engineering and Information Technology, Murdoch University, WA 6150, **Australia**

Physical and electrochemical characterization of Activated Carbon

The X-ray diffraction (XRD) pattern of the commercially bought activated carbon obtained from Calgon Carbon is shown in Fig. S1. The XRD showed two broad diffraction peaks of (002) and (100) planes at 23^{o} and 43^{o} degrees respectively. The diffraction pattern for this material matches well with the reported value [1]. The observed peak broadening implies an amorphous material with a random orientation. The ratio of the intensities of the two planes (I_{002}/I_{100} = 0.6) suggests the degree of highly ordered structure that may enhance the surface adsorption properties. The typical TEM micrograph of the activated carbon showed an amorphous in nature which is invariably seen for all the areas examined. The material exhibits nanostructure particles with an average size of 1-2 nm in size and the elemental composition analysis comprising C (95 %) and O (5%) as constituents.

Brunauer-Emmett-Teller (BET) analysis is an effective tool for evaluating the surface area of the activated carbon and its pore size distribution. This can be achieved from the nitrogen isotherms. N_2 adsorption-desorption measurement for the activated carbon is shown in Fig. S2. The material possesses a surface area of 700 m^2 g^{-1}, and it shows the characteristics of type – I isotherm according to the international union of pure and applied chemistry (IUPAC) classification [2]. A steep increase in low pressure, followed by a plateau at a relatively high pressure is a typical type I isotherm representing a material with microporous structure. The pore size distribution curve shows a narrow size distribution of pore sizes predominantly 1 – 3 nm.

The electrochemical performance of activated carbon was performed in 2 M NaOH under a standard three-electrode configuration with Pt wire and Hg/HgO as the counter and reference electrodes, respectively. Figure S3 (a) showed a typical cyclic voltammetry of the activated carbon exhibiting a quasi-rectangular shaped curve of electrochemical double layer capacitor (EDLC) behaviour in the region between 0 and -0.1 V. The cations and anions from the NaOH electrolyte are adsorbed on the activated carbon electrode layer during the anodic process while they are desorbed during the reverse scan [3]. The presence of pores associated with high surface area enhanced the electrolyte immersion on the electrode surface and its electrochemical activity [4]. The galvanostatic (charge-discharge) curves for this material is shown in Fig. S3 (b). The electrode potential varied from 0 to -1.0 V and the highly symmetric shape between the discharging and charging parts correlated well with the CV curve illustrating the double layer capacitive behaviour in a potential range of 1 V, showing reversibility of the material. The specific capacitance of activated carbon was calculated to be 135 F g^{-1}.

References

1. D. Yuan, J. Zeng, J. Chen, S. Tan, Y. Liu, N. Kristian and X. Wang, Synthesis of Hollow-cone-like carbon and its application as support material for fuel cells, J. Electrochem. Soc. 156 (2009) B 377 – B380.
2. S. – J. Zhang, H. – Q. Yu and H. – M. Feng, PVA – based activated carbon fibres with lotus root-like axially porous structure, Carbon 44 (2006) 2059 – 2068.
3. P. Staiti and F. Lufrano, Investigation of polymer electrolyte hybrid supercapacitor based on manganese oxide – carbon electrodes, Electrochim. Acta, 2010, **55**, 7436 - 7442.
4. L. Qie, W. M. Chen, Z. H. Wang, Q. G. Shao, X. Li, L. X. Yuan, X. L. Hu, W. X. Zhang and Y. H. Huang, Nitrogen-doped porous carbon nanofiber webs as anodes for lithium ion batteries with a super high capacity and rate capability, Adv. Mater. 24 (2012) 2047 – 2050.

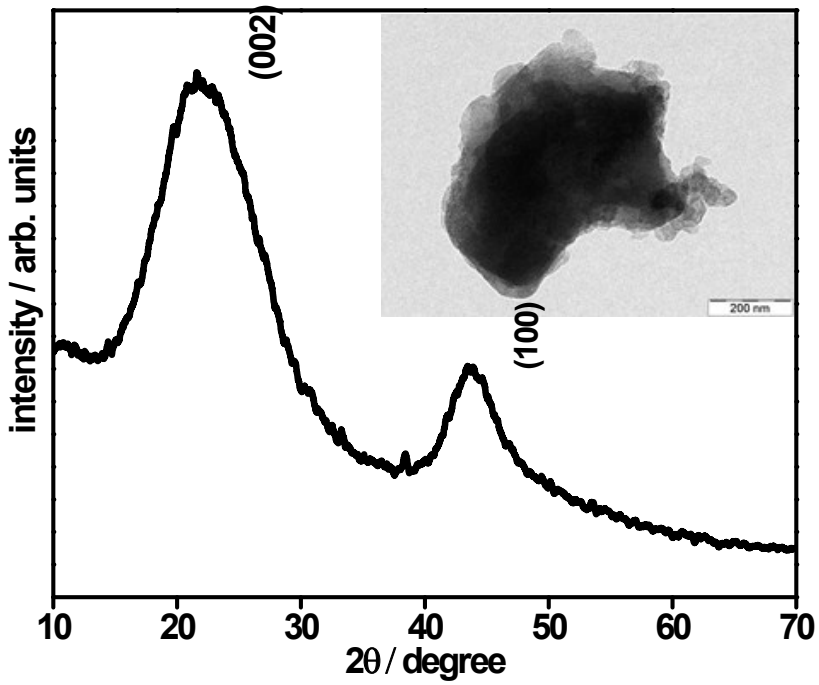

Figure S1 X-ray diffraction pattern of commercially available activated carbon. Inset shows the TEM imaging of the amorphous region.

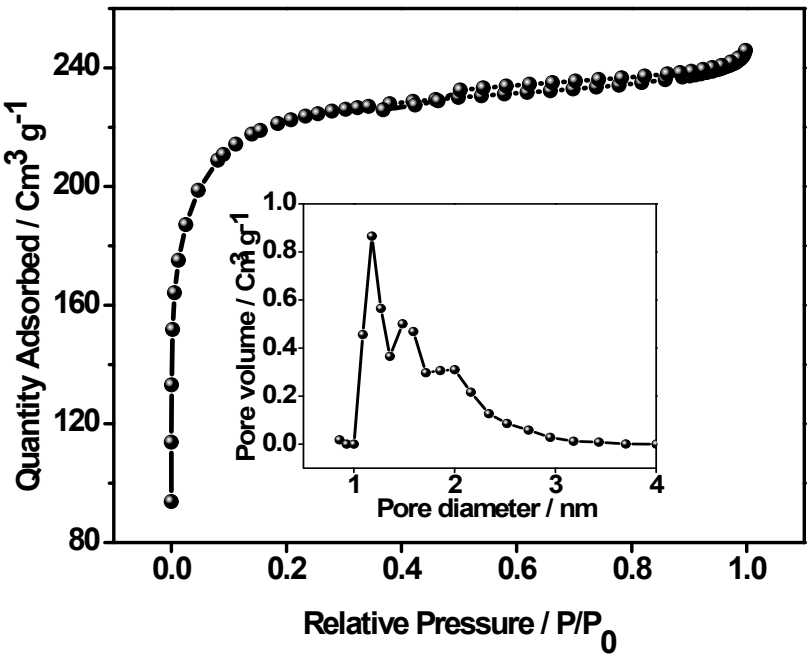

Figure S2 Nitrogen adsorption isotherm of activated carbon and the inset shows pore-width distribution.

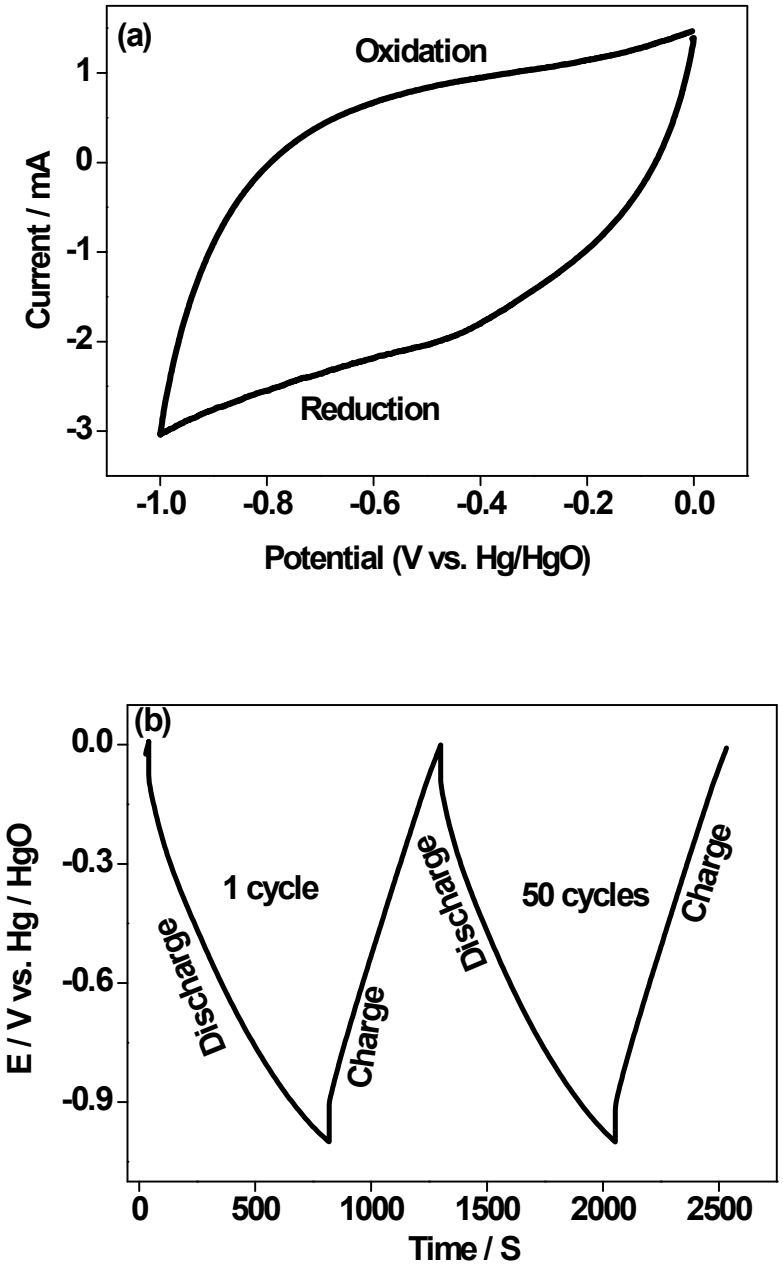

Figure S3 (a) Cyclic voltammogram (CV) for activated carbon (AC) negative electrode scanned at 2 mV s^{-1} and (b) corresponding galvanostatic (charge-discharge) curves for each electrode at 0.2 A g^{-1}. The plots are shown for the 1st and 50th cycles. Experiments are performed in a three electrode system in 2 M NaOH electrolyte.

Additional physical characterization of $CoMoO_4$

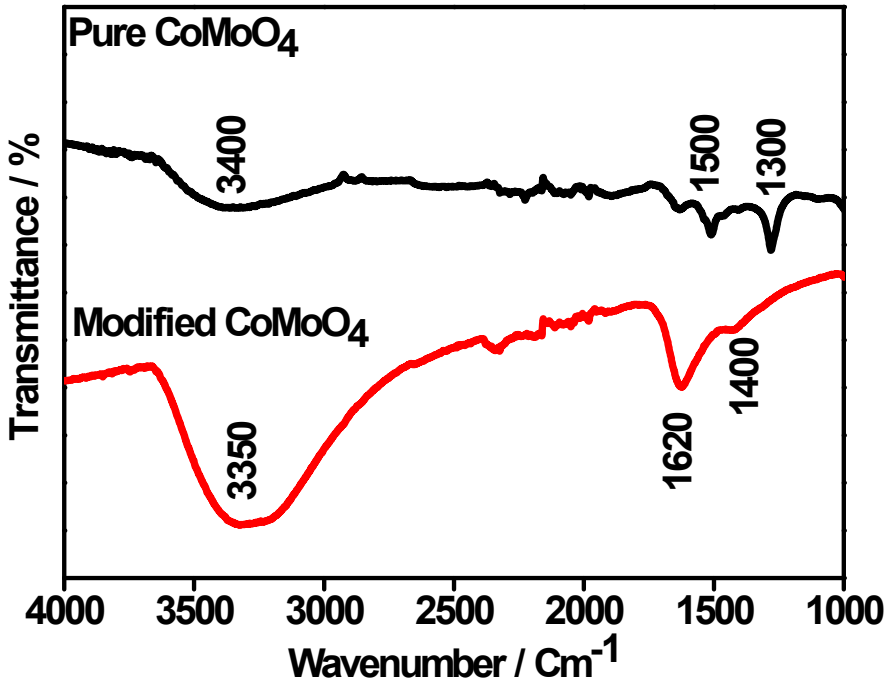

Figure S4 Mid infra-red region of transmittance spectra for the pure and modified $CoMoO_4$ material.

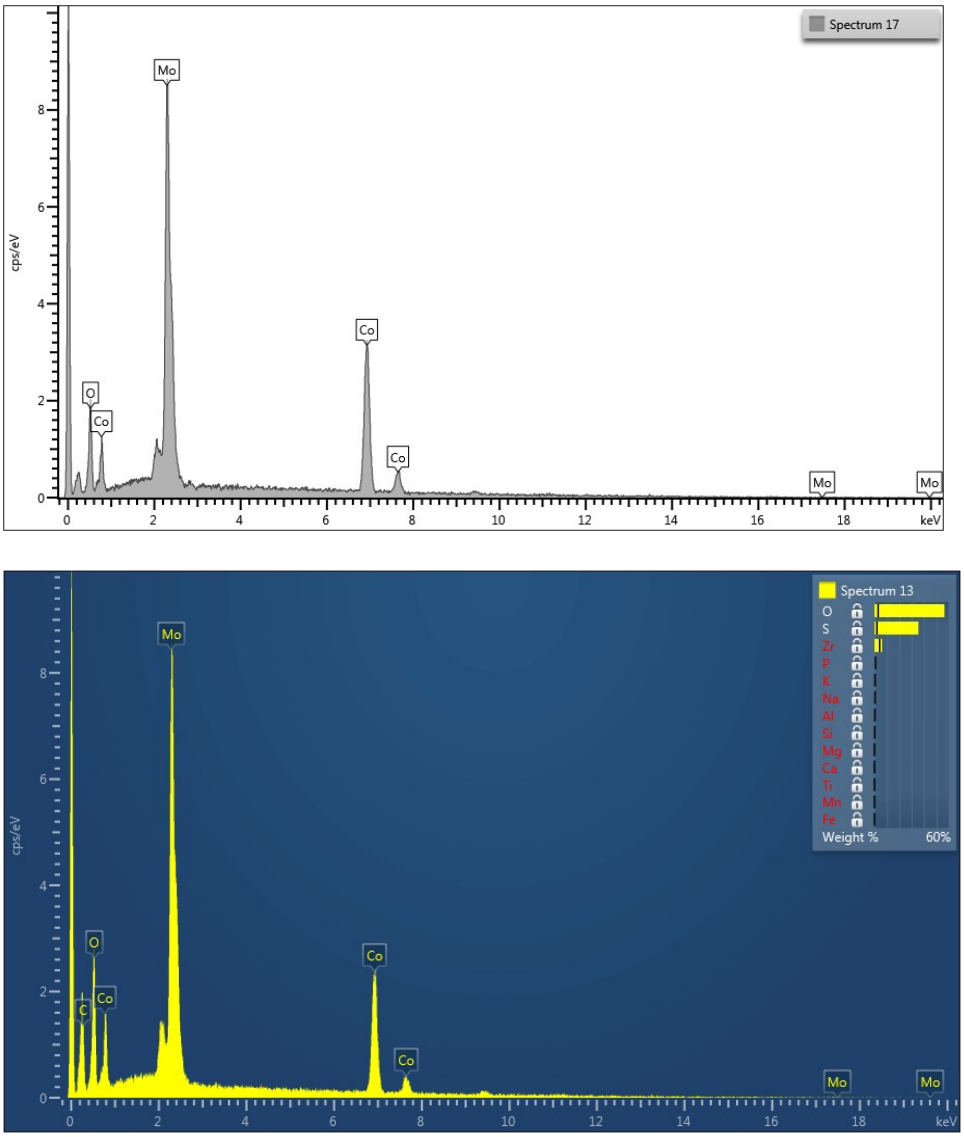

Figure S5 Field emission- scanning electron microscopy / energy dispersive spectral (FE-SEM/EDS) analyses of (top) pure and (bottom) modified $CoMoO_4$ with elemental compositions shown in the spectra. The presence of carbon is seen only for modified sample.

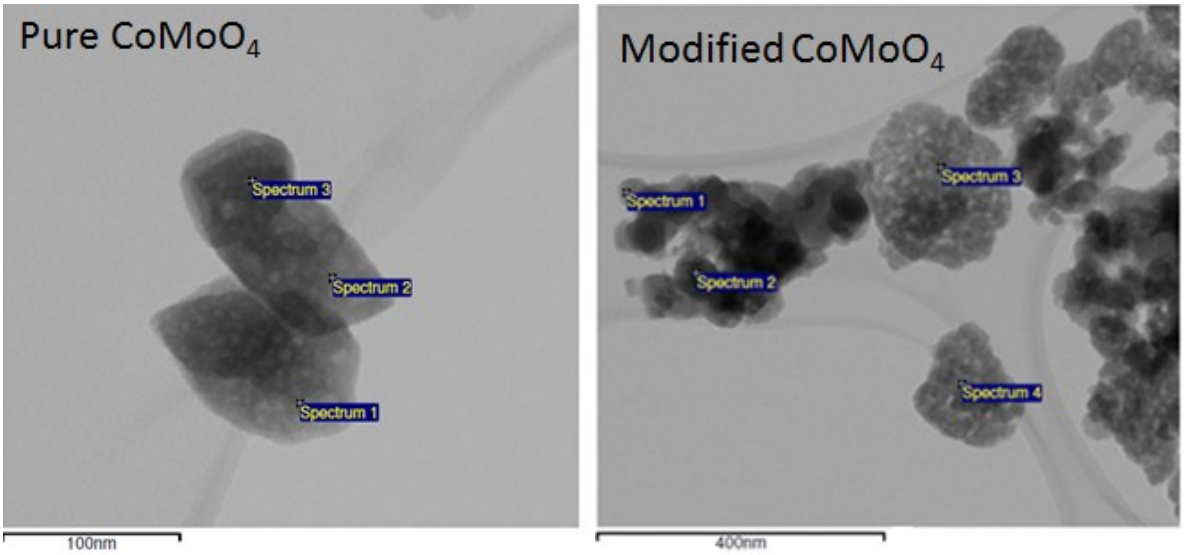

Pure $CoMoO_4$	**Co**	**Mo**	**O**	**Total**
1	17.19	52.08	30.72	100.00
2	16.57	52.61	30.82	100.00
3	16.51	52.66	30.83	100.00
Modified $CoMoO_4$	**Co**	**Mo**	**O**	**Total**
1	20.91	48.93	30.16	100.00
2	20.98	48.88	30.15	100.00
3	21.35	48.56	30.09	100.00
4	22.57	47.53	29.90	100.00

Figure S6 Transmission electron microscopy / energy dispersive spectral (TEM/EDS) analyses of pure and modified $CoMoO_4$ with typical elemental compositions obtained quantitatively from the regions indicated in the corresponding images.